Effects of Advanced Injection Strategies on In-cylinder Air-fuel Homogeneity of Diesel Engines

Pavlos Dimitriou[1a], Zhijun Peng[2*], Weiji Wang[1], Bo Gao[3], Matthias Wellers[3]

[1] School of Engineering & Informatics, University of Sussex, UK

[2] School of Engineering & Technology, University of Hertfordshire, UK

[3] AVL Powertrain UK, UK

[a] P.Dimitriou@sussex.ac.uk

Corresponding author

Zhijun Peng, School of Engineering & Design, University of Hertfordshire, Hatfield, AL10 9AB, UK

Email: Z.Peng2@herts.ac.uk

Abstract

Air-fuel mixing quality in the combustion chamber of a diesel engine is very critical for controlling the ignition and combustion quality of DI diesel engines. With a view to understanding the air-fuel mixing behavior and the effect of the mixture quality on the emissions formation, an innovative approach with a new quantitative factor of the in-cylinder air-fuel homogeneity named Homogeneity Factor (HF) has been used and its characteristics under various injection conditions have been analyzed with CFD simulation. By investigating the effect of advanced injection strategies to the homogeneity of the mixture and the emissions production, the study suggested that HF is highly affected by the pulse number of injections, injection timing and dwell angle between two injections. The more advanced the injection is taking place into the cylinder, the earlier the air-fuel mixing quality reaches at a high level. Although HF is not sufficiently precise by itself to reflect the emission formation, the results have demonstrated that most often the higher the homogeneity is available in the cylinder, the more NOx and less soot are to be formed.

Keywords

Diesel; homogeneity factor; air-fuel; mixing; NOx; soot; emissions; combustion

1. INTRODUCTION

In direct injection diesel engines, air-fuel mixing quality is of crucial importance for the combustion process. One of direct results is that uniform air-fuel mixture before the start of combustion can lead to low soot emission due to the avoidance of local fuel rich regions. However, this might cause high combustion temperature and high NOx emissions.

Many investigations have been reported with regard to optimizing the in-cylinder combustion and reducing the emissions formation. Most of them were targeted at improving the air-fuel mixing through advanced injection strategies or to vary the oxygen concentration by utilizing high level of Exhaust Gas Recirculation (EGR) and Variable Geometry Turbo-charging (VGT). However, little effort has been made to quantify the air-fuel mixing quality in the combustion chamber of diesel engines.

The primary investigations carried out on the effects of pilot injection in the combustion process can trace back in 1995 with works from Pierpont et al. (1) and Minami et al (2). They demonstrated that by having a pilot injection in the combustion process, the ignition delay could be reduced and this leaded to a lower heat release rate, with less NOx emissions and combustion noise.

Montgomery et al. (3) studied the effect of combining multiple fuel injection strategies and EGR for reducing NOx emissions. They showed that by combining EGR and multiple injections, NOx emissions could be further reduced by lowering the peak in-cylinder temperature. However, soot emissions were raised due to some increased temperature rich regions created as a result of the oxygen reduction within the cylinder. Diez et al. (4) carried out an investigation in a single cylinder optical diesel engine for the effect of split main injection (30%, 70%) with short dwell angle (11.8^{o} CA) and high EGR rates. The results showed improved indicated mean effective pressure (IMEP) and low NOx emissions. However, as the short time between two main injections the air-fuel mixing was poor, leading to high unburned hydrocarbon (HC) and soot emissions. Tow et al. (5) showed the importance of the dwell angle between injections in order to control soot formation and suggested that there would be an optimal dwell angle at a particular operating condition. Mobasheri et al. (6) studied the effect of dwell between two injections and proved that for his testing operating conditions, the optimum dwell angle between the injection pulses was around 20^{o}CA.

Badami et al. (7) studied the effect of fuel injection pressure. They achieved a reduction of particulate emissions up to 27% by increasing the injection pressure from 1300 to 1500 bars

in a HSDI diesel engine at 4000 rev/min. Their results also proved that particulate emissions can be reduced via enhanced spray penetration caused by the injection pressure increase. Hountalas et.al (8) investigated the effect of EGR temperature on a heavy duty DI diesel engine. They concluded that high EGR temperatures negatively affect the brake efficiency, peak combustion pressure and soot emissions. They also demonstrated that EGR cooling is favorable for retaining the benefits of low NOx emissions without sacrificing significantly the engine efficiency. Kwon et al (9) studied the effects of in-cylinder temperature and pressure on ignition delay of a DI diesel engine. They proved that ignition delay is highly affected by the in-cylinder temperature with low temperatures leading to increased ignition delays. Bobba et al. (10) demonstrated that an increase of the ignition delay from 3 to 15 crank angle degrees (CAD) led to a 95% decrease in the total in-cylinder soot mass of a heavy duty diesel engine operating at low temperature conditions.

While a number of researchers have been conducted for investigating effects of various injection strategies on air-fuel mixing, combustion process and emissions formation, there is very limited work for directly taking into account the specific information of fuel distribution in the chamber and particularly quantitative analysis of the air-fuel mixture. In 2002, Nandha and Abraham (11) defined a mathematical parameter named Degree of Heterogeneity (DOH)

for scaling the fuel distribution in the cylinder. They tested the definition using computational simulations to study the effects on the heterogeneity of the mixture for different operating conditions including multiple injection strategies and spray orientation.

For achieving a more directly quantitative parameter to classify the air-fuel mixing quality, Peng et al. (12) developed a Homogeneity Factor (HF) as a measure for the air-fuel mixing in the diesel engine. Then the factor was employed in CFD numerical simulation with KIVA-3V code for examining the influence of various operating parameters on in-cylinder mixing quality and it showed that the advance of injection timing does not always result in an increase of the air-fuel mixing homogeneity.

In this paper, the Homogeneity Factor will be further developed and be employed in AVL FIRE CFD code for exploring the effects of advanced injection strategies on the air-fuel mixing homogeneity, the combustion process and emissions formation. The paper is divided in the following categories; firstly the CFD model is validated compared to real engine test results. Secondly, simulations for five single injection strategies with different start of injection are performed. Then, twelve cases with split in the main injection in two pulses, different injection ratios and dwell angles are examined. Finally, the two cases with the best

combination of relatively low NOx and soot emissions are further analyzed by implementing a pilot injection of either 5% or 10% of the total injected fuel.

2. NUMERICAL METHOD

2.1. Sub-models. Numerical simulations were conducted by using AVL FIRE CFD code for Diesel combustion. The submodels employed in the code were chosen based on previous studies and it has been suggested that those sub-models are appropriate for high fuel pressure diesel combustion. In the code, the primary and secondary atomizations of the fuel spray are predicted using WAVE model (13), which has been widely used for high-speed fuel injections. WAVE model assumes that droplet size and breaking up time is related to the fastest-growing Kelvin-Helmholtz instability (14). The details of newly-formed droplets are predicted using the wavelength and growth rate of this instability. For heat-up and evaporation prediction of the droplets, Dukowicz evaporation model (15) is selected for the simulations with diesel fuel. The Dukowicz model determines the rate of the droplet temperature change by the heat balance, which states that the temperature transferred from the gas to the droplet supplies heat for its vaporization. For simulating the droplets' wall impinging process, the extended Kuhnke spray wall interaction model (16) was used. The

interaction is mainly depended on the droplet's velocity and diameter as well as the wall surface roughness and temperature.

The recently developed k-ζ-f model developed by Hanjalic, Popovac and Hadziabdic (2004) (17) was used for the evaluation of the turbulence effect in the combustion chamber. The ECFM-3Z (Extended Coherent Flame Model – 3 Zones) model (18) was applied for the combustion model of the simulations. The ECFM-3Z separates a computational cell in 3 zones in order to enable specific treatment for air fuel mixing, auto ignition, combustion and pollution formation processes. Finally, Zeldovich (19) and kinetic model (20) were implemented in the software for NOx and soot formation respectively. The kinetic model is a detailed chemical based reaction scheme for soot formation and oxidation calculation. The model used in AVL FIRE adopts a number of mechanisms suitable for IC-engine relevant fuels and provides an accurate approach for computationally soot formation calculation.

Table 1. Computational submodels

Break-up model	WAVE model (13)
Evaporation model	Dukowicz (15)
Wall interaction	Extended Kuhnke model (16)
Turbulent model	k-ζ-f model (17)
Combustion model	ECFM-3Z model (18)
NOx mechanism	Extended Zeldovich (19)

Soot model	Kinetic model (20)

2.2. Engine Specifications. A light duty single cylinder Ricardo Hydra diesel engine with compression ratio of 18.3:1 and swept volume of 499cm^3 is used in this study. A six-hole injector is placed centrally in the test engine to spray the fuel in the combustion chamber. The specifications for the engine and injection system are listed in Tables 2 and Table 3.

Table 2. Engine specifications

Displaced volume	499 cc
Stroke	86 mm
Bore	86 mm
Connecting rod	143.5 mm
Compression ratio	18.3:1
Number of valves	4
Inlet valve close	20° ABDC
Exhaust valve open	50° BBDC
Engine speed	2000rpm
Piston shape	Mexican hat style

Table 3. Fuel injection system specifications

Injection pressure	1,200 bar maximum
Number of nozzle holes	6
Nozzle hole diameter	0.169 mm

2.3. Computational Grid. The piston and the injector geometry parameters have been set in the software using the 2D Sketcher tool. The computational grid was generated and the model tested under various mesh sizes in order to make sure that results are grid independent. The final grid independent model, shown in Figure 1, consists of 42,052 and 72,052 hexahedral cells at TDC and BDC respectively.

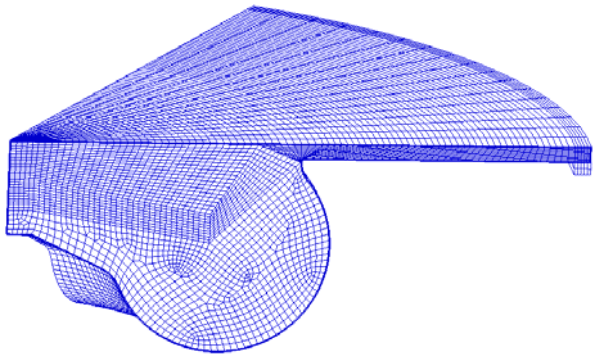

Figure 1. Computational grids at TDC.

2.4. Test Conditions. The tests were performed under the following air and fuel conditions.

Table 4. Initial air & fuel conditions

Intake air temperature	380 K
Intake air pressure	1 bar
Fuel temperature	350 K
Fuel injected	14.5 mg/cycle
Number of injections	1 to 3
Total injection duration	17.4^{o} CA
SOI 1st Main Injection	10^{o} CA BTDC

The tests were divided into three main categories. The first category includes five tests with single injection and different start of injection timings. The second category includes simulations performed by having two injections per cycle with different injection rates and dwell angles. Finally, the last category shows simulations performed for one pilot and two main injections in the cylinder. In order to make it clear, tests have been named according to the number of injections; A for 1 injection, B for 2 and C for 3 (1 pilot + 2 mains) respectively. Cases A are followed by a number declaring the CA degree where the injection starts. Cases B and C are followed by the percentage of the fuel injected during the first injection and then by the dwell angle in degrees in brackets which shows the angle between the end of first or second and the beginning of second or third injection respectively. For example, test

C5(10)70(10)25 defines that there were one pilot and two main injections into the cylinder. Pilot injection occurred with 5% of the total fuel injected during the pilot injection. The dwell angle between the pilot and the first main injection was 10^{o} CA. That means that the pilot injection finished at 10^{o} CA before the start of the first main injection. Following this, 70% of total fuel injected during the first main injection and the last injection of 25% of fuel was occurred after a dwell angle of 10^{o} CA.

Totally, 5 single and 16 multiple different injection arrangements have been considered. For single injection strategies the start of injection timing varies from 20^{o} CA BTDC to TDC in a step of 5^{o} CA. Split injection ratio varies from 10% to 30% for the second pulse and the variable dwell angle between the two main injections is from 5^{o} CA to 30^{o} CA. Two of the optimum split injection cases have been further analyzed by implementing a pilot injection of 5% and 10% of the total fuel injected at an earlier stage.

3. PARAMETER DEFINITION

In this paper, the mixing quality parameter used is one named Homogeneity Factor (HF) which was originally developed by Peng and Liu (12). The parameter has been modified for more accurate air-fuel mixing results within the cylinder. In the definition, it needs at first to

find the fuel difference in a calculated cell (e.g. Cell i), compared to the average equivalence ratio:

$$\frac{\Phi_i}{AFR_{st}+\Phi_i}\delta m_i - \frac{\Phi_0}{AFR_{st}+\Phi_0}\delta m_i = \frac{(\Phi_i-\Phi_0)AFR_{st}}{(AFR_{st}+\Phi_i)(AFR_{st}+\Phi_0)}\delta m_i \qquad (1)$$

Where AFR_{st} is the stoichiometric air-fuel ratio, Φ_0 is the average equivalence ratio, Φ_i is the equivalence ratio and δm_i is the mass of the mixture in the computational cell i.

The Total fuel amount in the cylinder is,

$$\frac{\Phi_0}{AFR_{st}+\Phi_0}M \qquad (2)$$

Where M is the total mass of the mixture.

Then, a parameter named Heterogeneity Factor (HeterF) can be expressed as,

$$HeterF(\theta) = \sum_{i=1}^{N_{cells}} \frac{\sqrt{(\Phi_i - \Phi_0)^2}\,\delta m_i}{2\Phi_0 M\left(1 + \frac{\Phi_i}{AFR_{st}}\right)} \qquad (3)$$

As the increased fuel amount in a cell actually comes from the decrease of fuel amount in other cells, the half of the standard deviation is used in the definition to reflect the non-uniformity more accurately.

Based on HeterF, the homogeneity factor (HF) can be derived for having a quantitative demonstration to the charge mixing quality.

$$HF(\theta) = (1 - HeterF(\theta))\% \qquad (4)$$

Compared to Nandha and Abraham's definition for Degree of Heterogeneity (DOH) which actually represents the standard deviation of the equivalence ratio normalized by the overall equivalence ratio (11), the HeterF (heterogeneity factor) is the standard deviation of fuel amount normalized by the overall fuel amount. This will be a more reasonable measure to the non-uniformity in the mixture.

4. MODEL VALIDATION

The CFD model was validated using experimental data conducted on a Ricardo 499cc single cylinder research engine with the specifications as listed in Table 2. The in-cylinder pressure of the engine was measured using a 0-250 bar range Kistler 6056 in-cylinder pressure sensor. The heat release rate was calculated based on the in-cylinder pressure and the in-cylinder volume. A Testo 350 XL portable emission analyzer was used for measuring the emissions formation.

Figure 2 shows the comparison between the predicted and measured in-cylinder pressure and heat release rates. The results are based on the assumption of uniform wall temperature 470 K for the cylinder wall and 570 K for the cylinder head and the piston top.

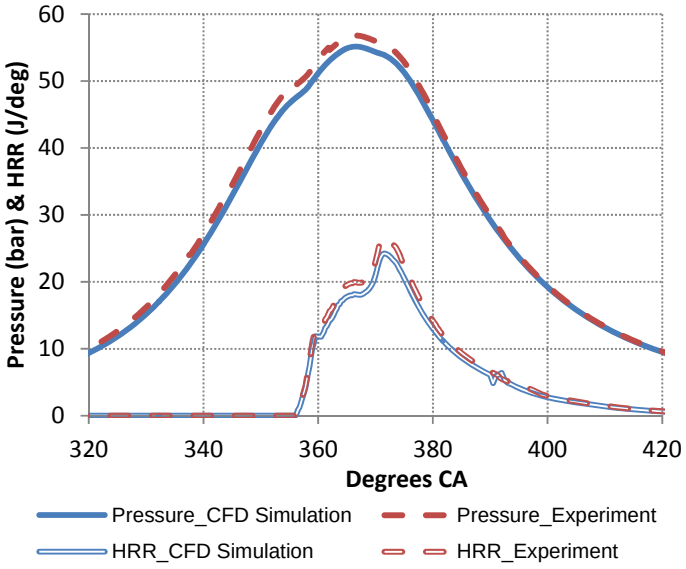

Figure 2. Comparison of simulated and measured in-cylinder pressures and heat release rates.

The CFD simulation trend for the in-cylinder pressure seems to be in reasonably agreement with the experimental measured values. There is only a slight pressure difference after the start of combustion which might be related to experimental uncertainties in input parameters to the computations such as the precise injection duration, start of injection and gas temperature at the IVC. On the other hand, the calculated heat release rate based on the experimental results seems to follow the same trend as in the simulation. However, the

calculated HRR is slightly higher than the simulation experiments and it seems to have a smoother drop after the end of the combustion.

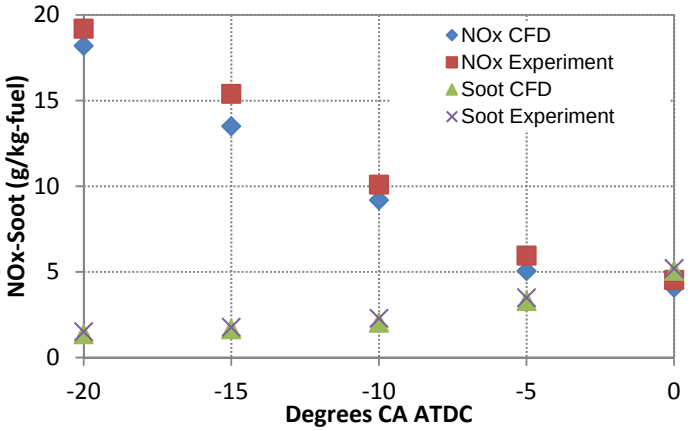

Figure 3. Comparison of simulated and measured NOx and soot emissions.

Figure 3 presents the comparison of NOx and soot emissions formation for single injection cases with different start of injection timings at 2000rpm. The simulation results are correspondent with the measured values. Thus, the model used in this study can provide enough confidence to the following simulation results with regard to the combustion process and emissions.

5. RESULTS AND DISCUSSION

5.1. Influence of Injection Timing. A single injection strategy study has been performed for understanding and validating the newly introduced homogeneity factor. The purpose of this study was to find the optimum start of the single injection based on the air-fuel homogeneity trend. Five single injection simulations were totally performed. The start of injection was varied from 20º CA BTDC to 0º CA BTDC while the fuel injection pressure and quantity were kept constant. Figure 4 shows that air-fuel mixture quality into the cylinder is directly influenced by the fuel injection timing. It is shown that as the SOI advances, a more homogenous locally fuel-lean in-cylinder mixture occurs at an earlier stage in the cylinder.

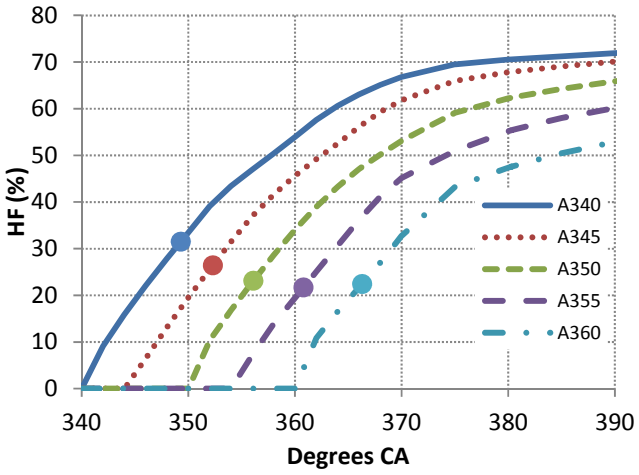

Figure 4. HF for single injection cases and HF (circle marker) at start of ignition.

Case A340 with SOI 20º CA BTDC has been further analyzed in Figure 5. It is shown that for the A340 case, where the fuel injection takes place at a very early stage, the in-cylinder pressure increases and the maximum value of Homogeneity Factor occurs closer to TDC. The early injection leads to longer ignition delay therefore more time is available to achieve a larger portion of pre-mixed mixture which leads to very high amount of temperature and thus to higher in-cylinder pressure.

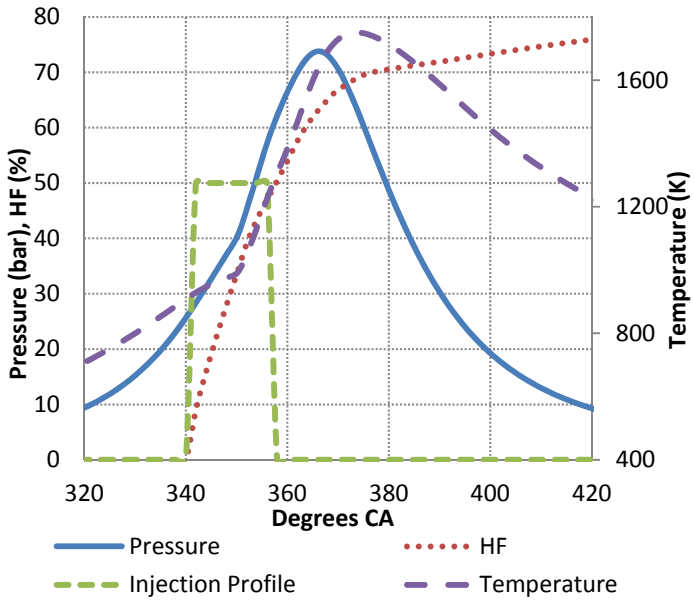

Figure 5. HF, injection profile, in-cylinder pressure and temperature for A340 case.

As the SOI is retarded, the ignition delay is shorter because of the higher in-cylinder temperature closer to TDC. Therefore the amount of pre-mixed combustion is reduced. This results in an increased amount of diffusion burning and lower peak in-cylinder pressure due to late initiation of the combustion process during the expansion stroke where the piston is descending after TDC.

Late fuel injection leads to fast pre-mixed combustion and less heat release as shown in Figure 6. However, this is compensated by the fast heat release of combustion in smaller volume near TDC. As a result, the peak HRR remained almost constant for cases A340, A345 and A350. However, this didn't occur for cases A355 and A360 where the heat release is slighty lower as the initiation of combustion took place at a late point where the in-cylinder was relatively lower and the piston was descending after TDC.

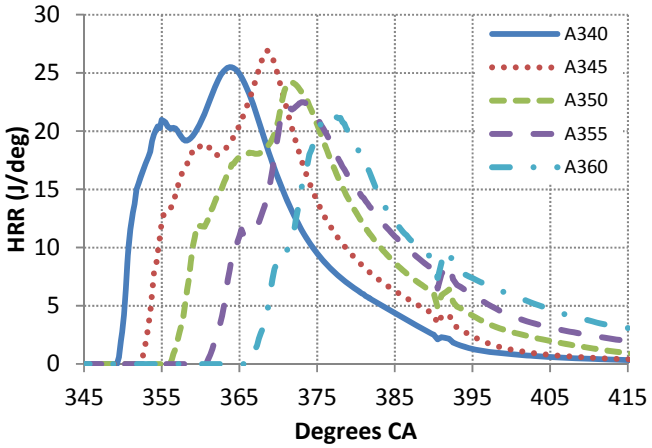

Figure 6. HRR graph for all A cases.

From the above study it can be concluded that the newly introduced homogeneity factor can be used as a useful measure for analyzing the air-fuel mixture and combustion process. The simplicity of its format makes the HF an extremely useful indicator for practical applications. It is shown that strategy A350 has the shortest ignition delay and a relatively high Homogeneity Factor at ignition timing and thus 10º CA BTDC is decided to be the SOI for the further experimental work.

5.2. Influence of Split Injection Strategies. In this section the effect of splitting the main injection into two pulses on the air-fuel homogeneity and emissions formation is presented.

In total twelve double injection strategies were simulated. In the first pulse, the fuel injected varies from 70% to 80% and 90% at 10º CA BTDC and the second pulse follows after 5º CA, 10º CA, 20º CA or 30º CA where the rest of the fuel is injected.

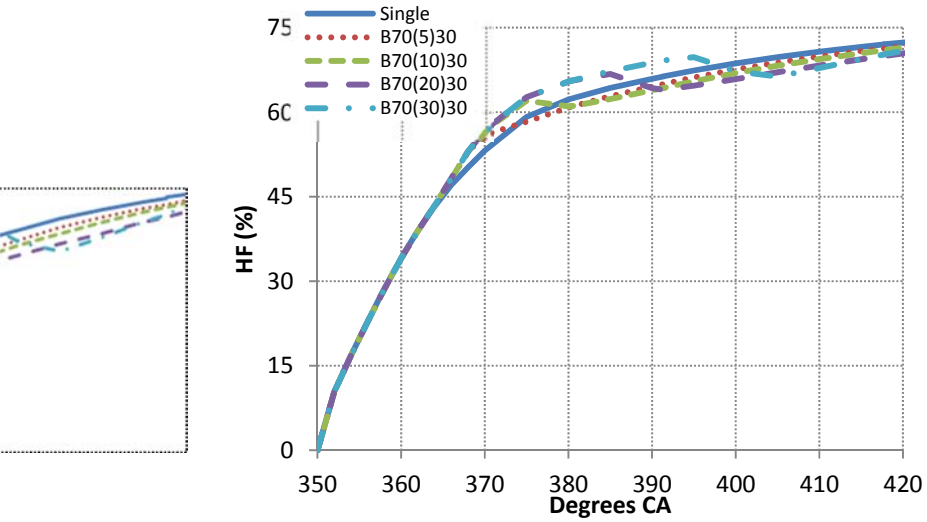

Figure 7. HF graph for B70 cases.

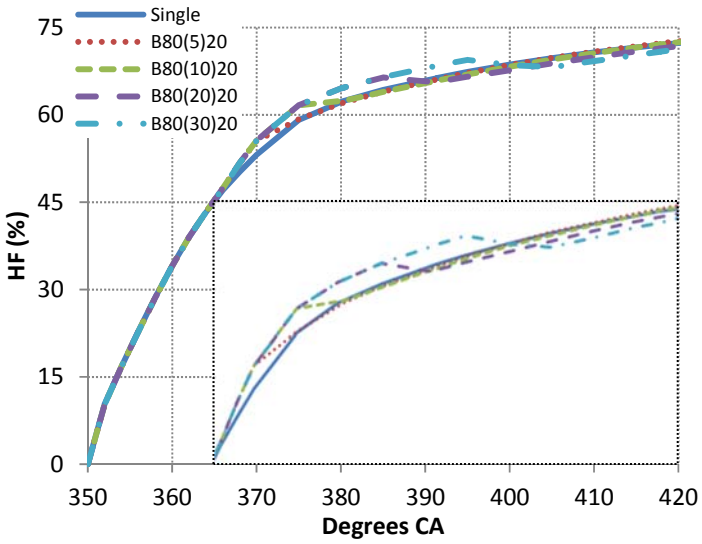

Figure 8. HF graph for B80 cases.

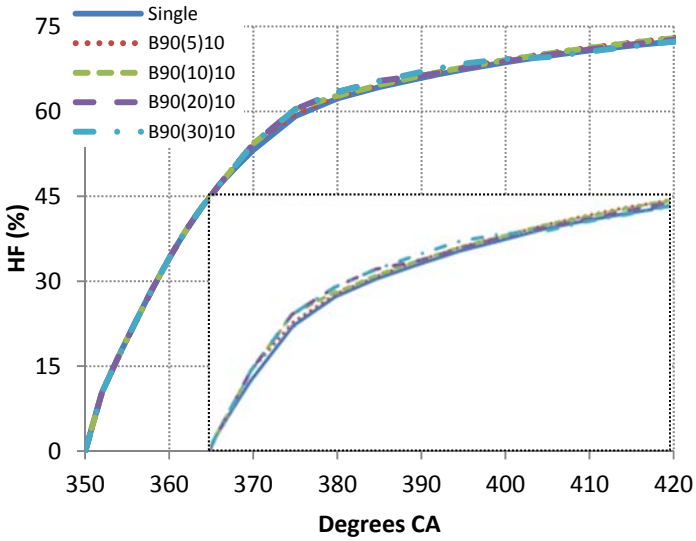

Figure 9. HF graph for B90 cases.

Figures 7, 8 and 9 present the air-fuel homogeneity over the cycle for 70%, 80% and 90% of fuel injected respectively during the first pulse. As shown in these figures the air-fuel homogeneity for the double injection cases is improved temporally at the point where the first injection ends. This is due to the available time for the fuel to be distributed with no more fuel diffusion compared to the single injection. However, when the second injection

starts, the Homogeneity Factor has not the same upward trend or it is even decreased in some cases. As it can be seen in Figures 7, 8 and 9 the longer the dwell angle is, the higher the homogeneity in between the two injections and also the bigger the drop of the homogeneity while the second injection occurs and at the end of the cycle. This can be caused by a poorer combustion with more residuals left within the cylinder. From the above figures it can be also noted that the higher the fuel quantity injected during the first pulse, the higher the homogeneity factor is after the end of the injections. This trend has different effects on NOx emissions which will be demonstrated in the following parts.

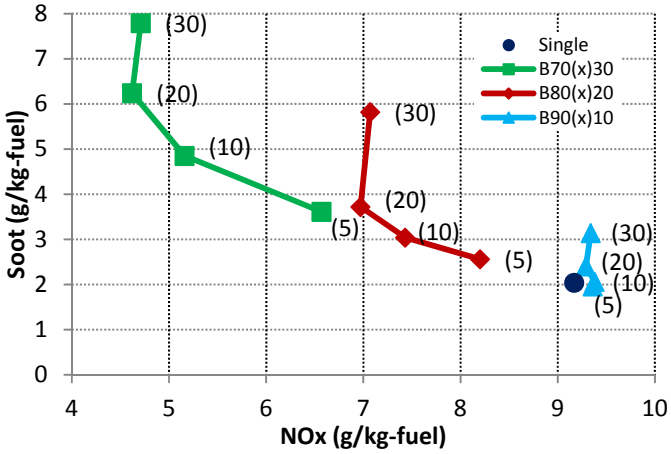

Figure 10. Soot-NOx trade-off, A350 and B cases.

Figure 10 illustrates the NOx and soot formation for the double injection strategies. It is clear, as expected, that double injection with 70% and 80% of fuel injected during the first pulse has a significant decrease in NOx formation. The NOx emissions are lower than the single injection strategy due to the greater control of the combustion process. The NOx formation is lower for cases with less fuel injected during the first pulse. This is in agreements with the Homogeneity Factor trend as a higher HF (cases with more fuel injected during the first pulse) will increase the rate of air-fuel mixing therefore a more complete combustion will take place which has a result to increase the NOx formation.

On the other hand, the split of the main injection in two pulses leads to higher soot formation. This is due to the fuel of the second pulse sprayed into burning regions caused from first injection, leading to a fuel-rich combustion. It is clear that the higher the fuel quantity during the second injection, the more soot is formed. In addition, the longer the dwell angle is, the more soot is formed due to the poor soot oxidation from the late initiation of the second pulse fuel combustion.

For the case with 90% of fuel injected during the first pulse, it seems that this splitting ratio is not able to reduce the NOx formation. However, for B90 cases with 5 and 10^{o} CA dwell, it seems that the soot formation has a slight reduction.

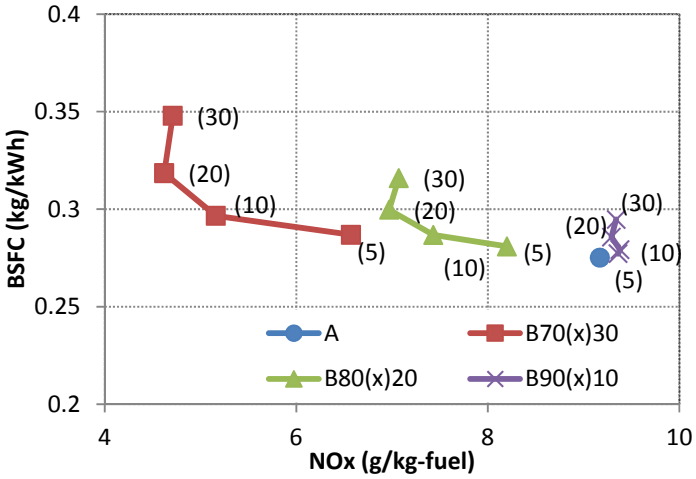

Figure 11. BSFC-NOx trade-off, A350 and B cases.

Figure 11 illustrates the Brake Specific Fuel Consumption over the NOx formation for the double injection strategies. It is shown that for B90 cases, the variations of both BSFC and NOx emissions are smaller than the other cases. From the above figure it can be concluded that the split injections shows minimal effect on the BSFC when the second injection follows at a short dwell angle and it has relatively lower fuel injection ratio compared to the main injection. Moreover, it can be noted that the higher the HF (strategies with more fuel injected during first pulse) results in reduction of BSFC. This is due to the improved air-fuel mixing quality which leads to an improved combustion therefore to less BSFC.

Figure 12 represents the Indicated Mean Effective Pressure vs. NOx formation of double injection strategies. It can be noted that the maximum IMEP levels can be obtained when having a short dwell angle between injections. In this case, the higher the fuel quantity injected during the first pulse leads to higher IMEP levels.

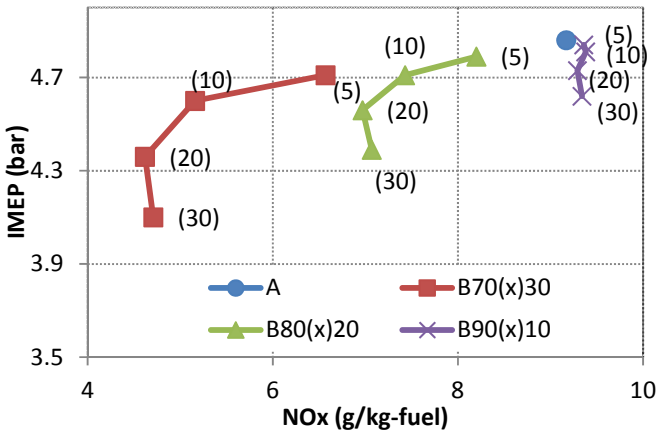

Figure 12. IMEP-NOx trade-off, A350 and B cases.

From all the above figures, cases B70 and B80 with 10^{o} CA and 20^{o} CA dwell have been picked due to the combination of relatively low NOx and soot formations. These cases have been further analyzed below based on the air-fuel mixing homogeneity.

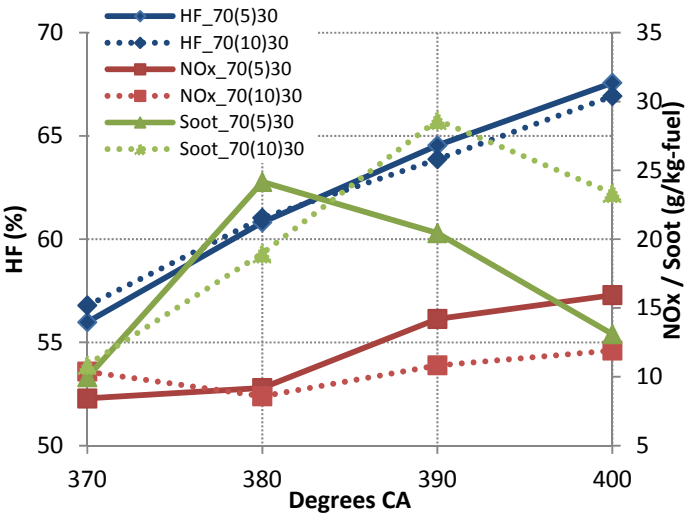

Figure 13. HF, NOx and soot emissions, B70 cases with 5 and 10° CA dwell angle.

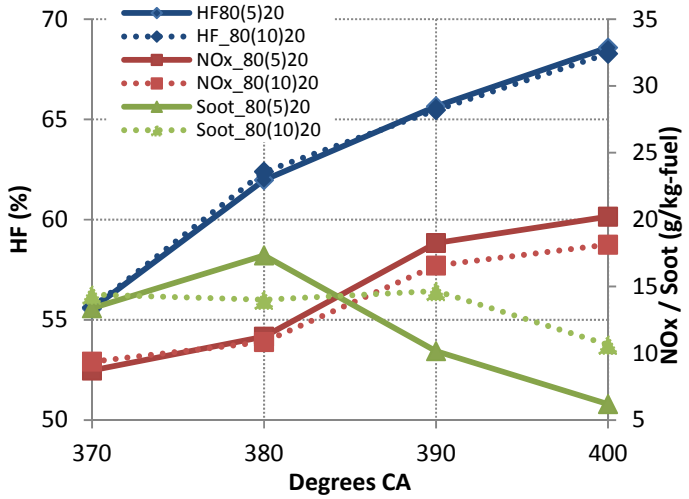

Figure 14. HF, NOx and soot emissions, B80 cases with 5 and 10° CA dwell angle.

Figures 13 and 14 compare the NOx and soot formation over the homogeneity factor at four critical points after the start of injection and combustion. In both figures the NOx and soot trend compared to the HF is similar. It can be mentioned that at 370^{o} CA, HF as well as NOx and soot are at the lowest levels. At 380^{o} CA, the HF climbs over 60% while the soot formation has a rapid increase for B70 cases and a lower one for B80 strategy. The NOx formation is still at low levels for both strategies. The NOx emissions are increased once the HF rises above 65%. It needs to be highly spotted from the above figures the NOx and soot variation based on the HF at different dwell angles. In Figure 13 is shown that the HF is slightly higher for the case with 10^{o} CA dwell than the one with 5^{o} CA at 370^{o} CA. At this point it can be also seen that NOx formation is slightly higher in 10^{o} CA case. Later at 390^{o} CA, the HF trend changes and the HF for 5^{o} CA case is a bit higher compared to the 10^{o} CA dwell case. At the same time the NOx formation trend also changes and the case of 5^{o} CA shows a higher NOx formation than the 10^{o} CA case. Likewise, soot formation for 10^{o} CA case is higher than the 5^{o} CA dwell angle.

From the Figures 13 and 14 it can also be concluded that the longer the dwell angle between the pulses, the less the NOx formation while there is an increase in the soot formation.

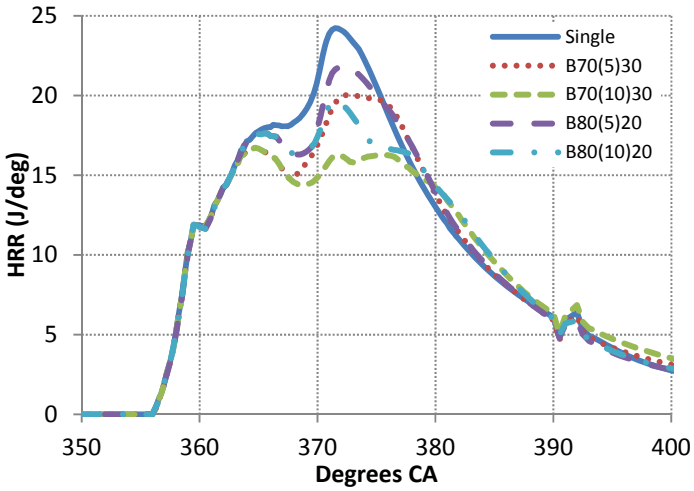

Figure 15. HRR graph, A350, B70 and B80 cases with 5 and 10° CA dwell angle.

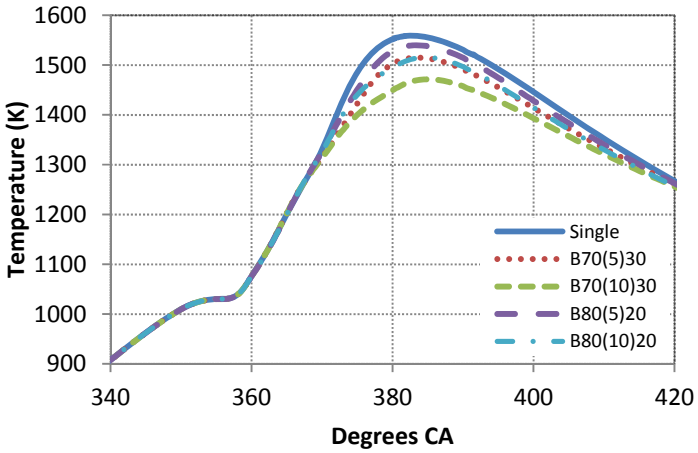

Figure 16. In-cylinder temperature graph, A350, B70 and B80 cases with 5 and 10^{o} CA dwell angle.

Finally Figures 15 and 16 show the heat release rate and in-cylinder temperature of the four cases compared to the single injection strategy. It can be noted that heat release curve of the single injection case varies from the HRR in the split injection strategies. The spit injections heat release graphs show two peaks formed by the two injections into the cylinder and an obvious valley in between. It seems that the second peak occurred due to the late combustion stage led to high in-cylinder temperatures and pressures. It can also be seen that the second HRR peak is highly affected by both dwell angle and the second's pulse injection quantity. The lower the dwell angle and fuel injection quantity during the second pulse, the higher the second HRR peak.

5.3. Influence of Pilot Injection. The B70 and B80 cases with 10^{o} CA degrees dwell angle have been chosen due to the combination of relatively low NOx and soot emissions with high IMEP and low BSFC values for further research by implementing a pilot injection. The pilot fuel injected varies from 5% to 10% with a dwell angle of 10^{o} CA and the fuel has been absorbed from the final injection of each strategy.

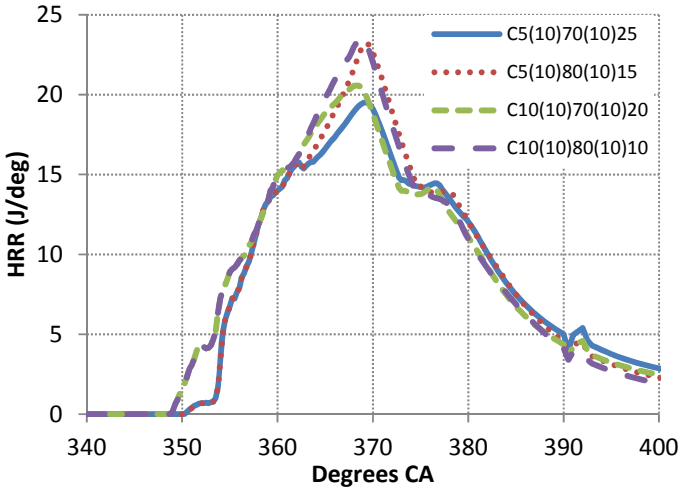

Figure 17. HRR graph, C cases.

Figure 17 shows that due to the early pilot injection into the cylinder the heat release rate inclines at an earlier stage. The maximum HRR reached in the C cases is higher than those in the split injection strategies (B cases).

Comparing Figures 15 and 17 one can see that by implementing a pilot injection into the cylinder at an early stage where the pressure and temperature are relatively low, it can lead to a high and sharp pressure and heat release increase. It is also shown in Figure 17 that the cases with the same quantity of fuel injected during the pilot pulse have similar and equal heat release trends. It can be concluded that pilot injection increases the heat release rate but at the same time the first main injection quantity plays a very important role on the percentage

increase. Figure 17 clearly shows that cases with 80% of fuel injected during the first main injection lead to a higher heat release rate compared to those with 70% regardless the pilot injection quantity.

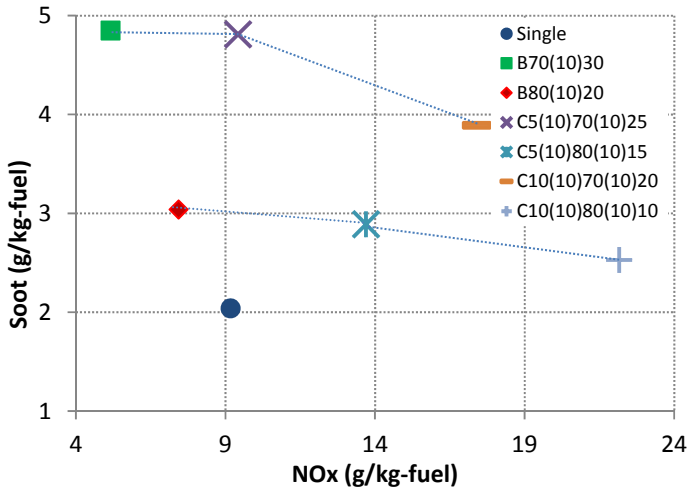

Figure 18. Soot-NOx trade-off, optimum A, B and C cases.

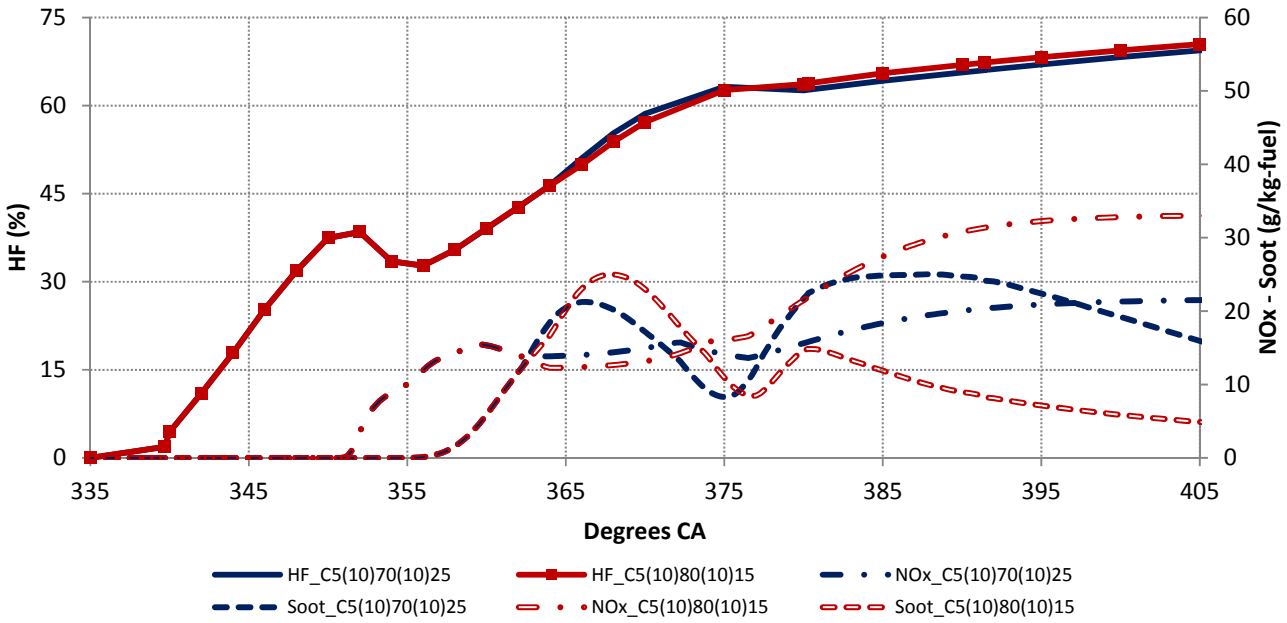

Figure 19. HF, NOx and soot emissions for C cases with 5% pilot injection.

As it had been shown before by splitting the main injection in two pulses, the NOx emissions can be dramatically reduced. However there is a soot penalty due the fuel rich combustion taking place during the second injection. From Figure 18, it can be observed that by implementing a pilot injection the NOx emissions are significantly increased instead of being reduced. The reason for this increase can be given by looking back to the heat release as in Figure 17 where the high HRR trend marks that the pilot injection took place at a very early

stage, leading to high temperatures and therefore to NOx increase. However, the soot emissions have been slightly reduced due to the fact that less fuel is injected during the second pulse compared with the B cases. Therefore, less rich fuel combustion and more soot oxidation takes place in the cylinder. It can be also noted that the cases with 5% of fuel injected during the first main injection have less NOx and more soot emissions than the 10% cases. This confirms the above justification for NOx and soot emissions variation.

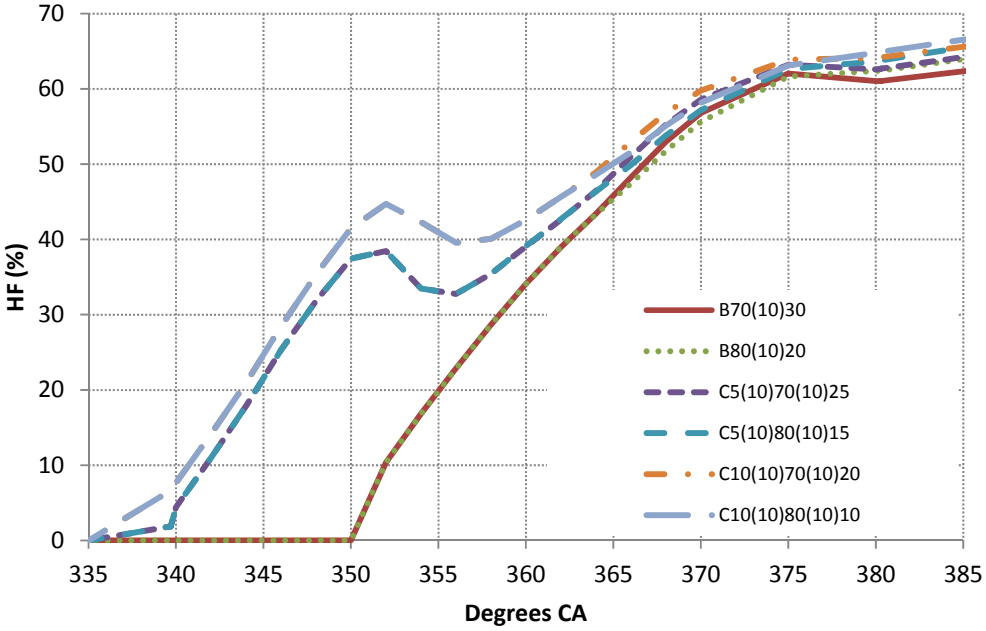

Figure 20. HF graph of C cases compared to B70 and B80 with 10°CA dwell angle.

The HF diagram in Figure 20 shows the air-fuel mixing quality into the cylinder for the C cases relative to B70 and B80 with 10º CA dwell angle. The lines for the same start of injection strategies are overlapping each other until the moment where some variation in the injection pulse occurs. It is shown that the HF at 5º CA BTDC, at the point where roughly the start of combustion for B cases occurs, is already at high rates due to the pilot injection took place earlier in the cylinder. The HF for the 10% of fuel pilot injected has an almost 10 unit higher factor than those of 5% of fuel pilot injected. This is due to the earlier start of injection, as the pilot injection in cases with 10% fuel started almost 1º CA in advance. Looking at this high air-fuel homogeneity at the initiation of combustion after the first main pulse, it can be definitely justified the expected NOx increase compared with B cases as shown previously. Moreover, it can also be noted from the above figures that the HF for C cases remain at higher levels compared with B cases until a very late state of combustion. This can conclude that there is optimal and more complete fuel combustion in the cylinder with less residuals and therefore higher homogeneity. Finally, results shown in Figure 20 once again prove the importance of first main injection to the air-fuel homogeneity levels and as a result to the emissions formation. It can be seen that the cases with 70% of fuel injected during the first pulse have higher HF at the end of the main injection as in the cases with 80% injection still occurs. However after a while when first main injections in both

70% and 80% cases are over, the HF for 70% decreases and drops below the 80% cases which perfectly justifies the higher NOx emissions.

Finally Figure 19 represents the HF trend over the NOx and soot formation for C cases with 5% pilot injection. It can be sees that homogeneity for the case with 70% of fuel injected during the first main injection is temporarily improved after the end of the first main injection compared to the other case where there is still fuel injection taking place for a few more degrees. However, almost at 15^{o} CA ATDC, the HF for C5(10)80(10)15 is getting higher than the C5(10)70(10)25 case. This happens due to the less amount of fuel injected during the second main injection which does not deteriorate in-cylinder mixing too much. Another point worth to be mentioned is the identical behavior of the HF and NOx emission trend. At the point where the HF for the C case with 70% fuel for the first main injection is getting higher compared to the other case, the emissions formation is also higher. When the trend of this case goes below the C case with 80% of fuel during the first main injection, the NOx trend is also decreased and moves at lower level than C5(10)70(10)25 case. Vice-versa happens for the soot emissions where is lower for the cases with higher HF at any points in the cycle.

6. CONCLUSION

In this paper, a recently developed parameter called “Homogeneity Factor” has been applied in order to study the effect of air-fuel mixing quality to the combustion characteristics and emission formation of a single cylinder DI diesel engine. The study of the air-fuel mixing behavior is of great importance for understanding the engine’s performance and emissions behavior. The HF parameter can be an extremely helpful tool for finding the correlation between the in-cylinder mixing quality and the emissions formation. Simulations were performed for various single injection timings as well as split and multiple injection strategies. The main findings of this work can be summarized as follows:

- Air-fuel mixing quality in the cylinder is directly influenced by the fuel injection timing. As the SOI advances, a more homogenous fuel-lean mixture occurs at an earlier stage in the cylinder.

- Split injection can be used to improve the air-fuel mixture temporally at the point where the first injection ends. This is due to the available time when the fuel has to be distributed into the cylinder with no more fuel diffusion compared to the single injection.

- Although split injection can be used to improve the air-fuel mixture locally, the homogeneity level is dropped when the second injection takes place. This leads to reduction of NOx emissions but to a rapid increase of the soot formation.

- The HF drop at the start of the second main pulse in a split injection strategy is mainly affected by the dwell angle between the two injections. It seems that the smaller the dwell angle is the less the HF falls which leads to more NOx and less soot formation.

- The pilot injection leads to an improved air-fuel mixing quality at the point where the first main injection occurs. However, the early in-cylinder fuel injection and the high HF lead to high hear release rate and NOx formation.

- All the simulations performed in this paper clearly show that a high HF leads to a more complete combustion which has as a result to increase the NOx and reduce soot emissions.

The findings of this paper demonstrated that HF is a very useful indicator for studying and understanding in-cylinder air-fuel mixing and emissions formation behavior. However, other in-cylinder characteristics such as residual gases as well as temperature and pressure distribution within the cylinder that cannot be captured by the HF should be taken into account for the performance and emissions formation of a DI diesel engine. Any future work

should include finding a correlation between HF, residual gases, temperature distribution and injection characteristic variables.

ACKNOWLEDGMENTS

This work was produced in the framework of SCODECE (Smart Control and Diagnosis for Economic and Clean Engine), a European territorial cooperation part-funded by the European Regional Development Fund (ERDF) through the INTERREG IV A 2 Seas Programme.

The authors acknowledge the AVL Company to provide computational resources for this research.

REFERENCES

(1) Pierpont, D. A., Montgomery, D. T. and Reitz, R. D., "Reducing particulate and NOx using multiple injection and EGR in a D.I. diesel", SAE paper 950217, 1995.

(2) Minami, T., Takeuchi, K. and Shimazaki, N., "Reduction of Diesel Engine NOx Using Pilot Injection", SAE paper 950611, 1995.

(3) Montgomery, D. T. and Reitz, R. D., “Effects of Multiple Injections and Flexible Control of Boost and EGR on Emissions and Fuel Consumption of a Heavy-Duty Diesel Engine”, SAE paper 2001-01-0195, 2001.

(4) Diez, A. and Zhao, H., “Investigation of Split Injection in a Single Cylinder Optical Diesel Engine”, SAE paper 2010-01-0605, 2010.

(5) Tow, T., Pierpont, D., and Reitz, R., “Reducing Particulate and NOx Emissions by Using Multiple Injections in a Heavy Duty D.I. Diesel Engine”, SAE Technical Paper 940897, 1994.

(6) Mobasheri, R., Peng, Z., Mirsalim, S. M., “Analysis the effect of advanced injection strategies on engine performance and pollutant emissions in a heavy duty DI-diesel by CFD modeling”, Int. J. Heat Fluid Flow (2012), 33, 1 59-69, 2012.

(7) Badami, M., Nuccio, P., and Trucco, G., “Influence of Injection Pressure on the Performance of a DI Diesel Engine with a Common Rail Fuel Injection System”, SAE Technical Paper 1999-01-0193, 1999.

(8) Hountalas, D.T., Mavropoulos. G.C., Binder, K.B., “Effect of exhaust gas recirculation (EGR) temperature for various EGR rates on heavy duty DI diesel engine performance and emissions”, Energy, 33, 2 272-283, 2008.

(9) Kwon, S., Arai, M., Hiroyasu, H., “Effects of Cylinder Temperature and Pressure on Ignition Delay in Direct Injection Diesel Engine”, The Japan Institute of Marine Engineering, Vol. 18, No.1, 1990.

(10) Bobba, M. Genzale, C., Musculus, M., “Effect of Ignition Delay on In-cylinder Soot Characteristics of Heavy Duty Diesel Engine Operating at Low Temperature Conditions”, SAE Int. J. Engines, 2(1):911-924, 2009.

(11) Nandha, K. and Abraham, J., “Dependence of Fuel-Air Mixing Characteristics on Injection Timing in an Early-Injection Diesel Engine”, SAE Technical Paper 2002-01-0944, 2002.

(12) Peng, Z., Liu, B., Tian, L., and Lu, L., “Analysis of Homogeneity Factor for Diesel PCCI Combustion Control”, SAE Technical Paper 2011-01-1832, 2011.

(13) Reitz, R. D., “Modeling Atomization processes in High-Pressure Vaporizing Sprays”, Atomization and Spray Technology, 3:309-337, 1987.

(14) Kelvin, L., Thomson, W., “Hydrokinetic solution and observations”, Philosophical Magazine 42. Pp 362-377, 1871.

(15) Dukowicz, J. K., “A particle-fluid numerical model for liquid sprays”, Journal of Computational Physics, 1980, 35(2):229-253.

(16) Khunke, D., “Spray/Wall-Interaction Modelling by Dimensionless Data Analysis”, Shaker Verlag, 2004, ISBN 3-8322-3539-6.

(17) Hanjalic, K., Popovac, M., Hadziabdic, M., “A robust near-wall elliptic-relaxation Eddy-viscosity turbulence model for CFD”, Int. J. Heat and Fluid Flow (2004), 25,6:1047-1051.

(18) Colin, O., Benkenida, A., “The 3-zones extended coherent flame model (ECFM3Z) for computing premixed/diffusion combustion”, Oil & Gas Science and Technology,2004, Rev. IFP. 59, 6, str. 593-609.

(19) Heywood, J. B., “Internal Combustion engine Fundamentals”, McGraw-Hill. Inc., ISBN 0-07-028637-X, 1988.

(20) Hiroyasu, H., Nishida, K., “Simplified Three Dimensional Modeling of Mixture Formation and Combustion in a DI Diesel Engine”, SAE paper 890269, 1989.

DEFINITIONS, ACRONYMS, ABBREVIATIONS

ATDC	After Top Dead Centre
BDC	Bottom Dead Centre

BSFC	Brake Specific Fuel Consumption
BTDC	Before Top Dead Centre
CA	Crank Angle
CFD	Computational Fluid Dynamics
CFM	Coherent Flame Model
DOH	Degree of Heterogeneity
ECFM-3Z	Extended Coherent Flame Model – 3 Zones
EGR	Exhaust Gas Recirculation
EVO	Exhaust Valve Opening
HF	Homogeneity Factor

HeterF	Heterogeneity Factor
HRR	Heat Release Rate
HSDI	High-Speed Direct Injection
IMEP	Indicated Mean Effective Pressure
IVC	Inlet Valve Closure
NOx	Oxides of Nitrogen
PCCI	Premixed Charge Compression Ignition
ppm	parts per million
SOI	Start of Injection
TDC	Top Dead Centre
HC	Hydrocarbons
VGT	Variable Geometry Turbocharger